



ELSEVIER

Thermochimica Acta 284 (1996) 309–324

thermochimica
acta

Calorimetric investigation on liquid crystals of deoxyribonucleic acid in concentrated solutions

Akihiro Kagemoto*, Motonao Nakazaki, Satoshi Kimura,
Yoshihiko Momohara, Ken-ichi Ueno, Yoshihiro Baba

*Laboratory of Chemistry, Department of General Education, Osaka Institute of Technology, Asahi-ku,
Osaka 535, Japan*

Received 2 March 1994; accepted 4 November 1994

Abstract

The phase states of DNA in concentrated solutions have been studied by simultaneous measurement using differential thermal analysis (DTA) and a visible optical method (He–Ne gas laser, $\lambda_0 = 633$ nm) equipped with a computer, and using a polarization microscope equipped with a hot stage, and IR spectra.

From the polarization microscope results, DNA below a concentration of 2.00 wt% showed an isotropic phase; in the concentration range 3.00–5.00 wt%, DNA showed an anisotropic phase; and in concentrations above 6.00 wt%, DNA showed an anisotropic phase with a distinct birefringence from the measurement of the refractive index at 298 K, i.e. at concentrations above 6.00 wt% DNA forms a liquid crystal phase state.

In order to obtain information about the mechanism of formation of the liquid crystal of DNA, IR spectra for solutions containing 10.0 wt% of DNA and Mg^{2+} ion have been measured at room temperature. DNA does not form liquid crystals in the presence of Mg^{2+} ion. Therefore, an electrostatic interaction between the PO_4^- group in the main chain of DNA and the Mg^{2+} ion plays an important role in blocking the formation of the liquid crystal. Thus, it is suggested that DNA in concentrated solutions forms liquid crystals by a molecular orientation arrangement based on the repulsive force between the negative PO_4^- groups in the main chain of DNA.

The change in the enthalpy of formation of the liquid crystal of DNA has been estimated to be about -2.8 kJ mol $^{-1}$ of nucleotide, by considering the change in the intensity of transmitted laser light, using the DTA apparatus equipped with a laser.

Keywords: DNA; Calorimetry; Spectrometry; Liquid crystal; Order–disorder transition; Change in enthalpy

* Corresponding author.

1. Introduction

One of the most interesting areas of research in biopolymers is the interaction between DNA and small molecules. Many investigations concerning the change in conformation of DNA and the interactions between DNA and small molecules have been carried out in dilute solutions by various experimental methods.

In previous papers [1–8], the thermodynamic quantities based on the interactions between DNA and small molecules such as protein [1,2], metallic ions [3,4], drugs [5,6] and dyes [7,8] in dilute solutions have been studied by means of microcalorimetry and spectrophotometry.

However, it is very difficult to determine how the behaviors of DNA in dilute solution are related with the development of functions in vivo such as the transcription and replication of heredity. Because DNA in vivo exists as solutions with a concentration of 70 vol% as bacterial nucleoids [9], to obtain a more realistic understanding, DNA should be studied in concentrated solutions.

Recently, it has been reported that DNA solutions of various concentrations have shown liquid crystals [10–15], and also that the poly(A)·Poly(U) duplex formed by an equimolar mixture of poly(A) and poly(U) in concentrated solutions forms liquid crystals such as spherical and layered liquid crystals, depending on the concentration [16–18].

No information, however, has been obtained for the change in enthalpy on liquid crystal formation of DNA. In this study, DNA solutions with various concentrations have been investigated by means of a simultaneous measurement by differential thermal analysis (DTA) and a visible optical method (He–Ne gas laser; $\lambda_0 = 633$ nm) equipped with a laser, and also using a polarization microscope, an infrared spectrophotometer, and/or the refractive index.

We will discuss the mechanism of the liquid crystal formation of DNA by combining the results of calorimetry with those of spectrophotometry.

2. Experimental

2.1. Materials

The Deoxyribonucleic acid (DNA) used in this study was calf thymus DNA containing 42% of guanine–cytosine base pairs, purchased from Sigma Chemical Co., USA.

The sample was used after purification several times according to the normal method, i.e. phenol–chloroform extraction to remove protein [19]. The concentration of DNA was determined by the phosphorus analysis method [20].

The solvent used to adjust to pH 7.00 was 1.0×10^{-2} mol dm⁻³ phosphate buffer solution. The water used to prepare the buffer solutions was passed through an inverse osmotic membrane, deionized by an ion-exchange resin, and finally, distilled.

Samples of solutions with various concentrations of DNA were used about three weeks after preparation.

2.2. Apparatus and procedure

The apparatus used in this study was a differential scanning calorimeter (DSC; DASM-4) and a differential thermal analysis (DTA) set-up equipped with laser (He–Ne gas laser; $\lambda_0 = 633$ nm), similar to that reported previously [16,21], except that the equipment was connected with a computer. The analog signals corresponding to the thermal change detected from the DTA apparatus and the laser transmittance passing through the sample and reference cells were converted to digital signals by an A/D converter (AB 98-30B; ADTEK System Science Co. Ltd., Japan). Consequently, the change in enthalpy from the area of the DTA thermograms and the intensity of the laser transmittance inputted to the computer can be analyzed simultaneously.

The change in enthalpy estimated from the areas of the DTA curve was determined using the value $2.42 \times 10^{-2} \text{ J cm}^{-2}$ which was estimated from standard samples such as benzophenone, naphthalene and benzil.

The microscope used in this study was a polarization microscope (XTP-11, Nikon Co. Ltd., Japan). The temperature dependence of the phase states of DNA in concentrated solutions was measured by the polarization microscope using a hot stage.

The heating rates employed for the DTA equipped with a laser, DSC, and the polarization microscope with hot stage were about 1 K min^{-1} , respectively.

IR spectra were measured with a FT/IR 5000, JASCO spectrophotometer. The IR cells used were made of CaF_2 optical crystal (GL Science, Inc., Japan), and the IR spectral measurements for DNA solutions of concentration 10.0 wt% were carried out at room temperature. In this case, a polypropylene film was used as a spacer to maintain a light-path length of a μm .

The refractive index of DNA was measured at room temperature using a refractometer (T. Atago Co. Ltd., Japan).

3. Results and Discussion

3.1. Polarization microscope

The phase states of DNA over the concentration range 1.00–10.0 wt% were observed at room temperature using a polarization microscope. The typical phase states at various concentrations are shown in Fig. 1(a)–(c), respectively. As seen in Fig. 1(a), DNA at concentrations below 2.00 wt% exhibits an isotropic phase. In the concentration range 3.00–5.00 wt%, DNA exhibits an anisotropic phase as shown in Fig. 1(b); and finally, in concentrations above 6.00 wt%, DNA exhibits an anisotropic phase like a liquid crystal as shown in Fig. 1(c). From these results, the DNA molecule gradually becomes an ordered structure, with arrangement of its molecular orientation, and seems to form stable liquid crystals.

3.2. Refractive index

In order to confirm the various phase states of DNA, the refractive indices for DNA solutions with various concentrations were measured at 298 K, and the results

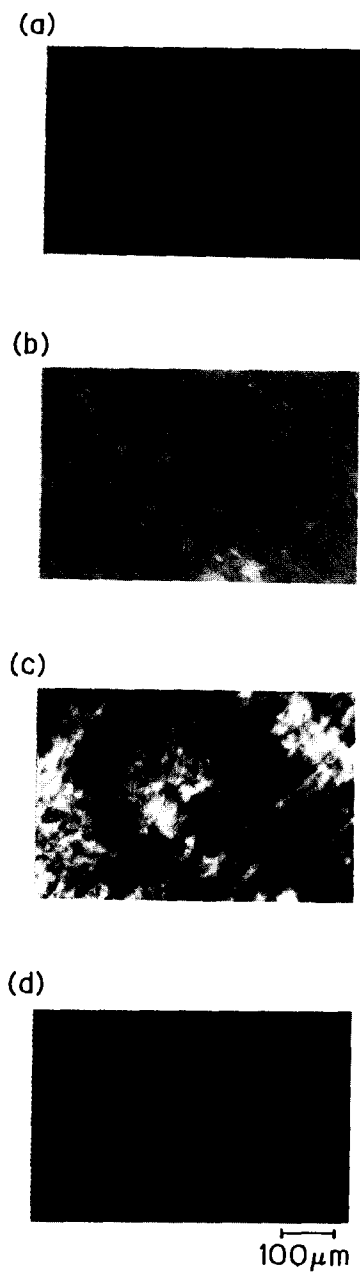


Fig. 1. Polarizing microphotographs of the phase states of DNA solution with various concentrations of DNA at room temperature: (a) DNA concentration 1.00–2.00 wt%; (b) DNA concentration 3.00–5.00 wt%; (c) DNA concentration 6.00–10.0 wt%; (d) DNA concentration 10.0 wt% containing Mg^{2+} ion.

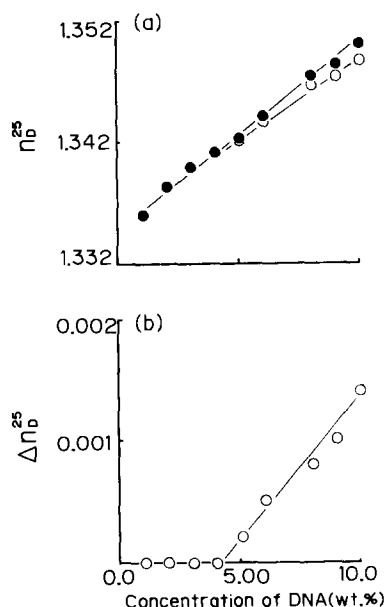


Fig. 2. Plots of (a) refractive index n_D^{25} , parallel to the prism plane (○), and perpendicular to the prism plane (●). (b) Birefringence Δn_D^{25} as the difference between refractive indices parallel and perpendicular to the prism plane.

obtained are shown in Fig. 2. Fig. 2(a) shows the plot of the refractive index n_D^{25} against various concentrations of DNA. As seen in Fig. 2(a), deviations of n_D^{25} both parallel and perpendicular to the prism plane appear from a concentration of 5.00 wt% of DNA, becoming larger with increasing concentration of DNA, i.e. these deviations correspond to the birefringence accompanying formation of the liquid crystal. Fig. 2(b) shows a plot of the birefringence Δn_D^{25} , the difference between the refractive indices parallel and perpendicular to the prism plane, against each concentration of DNA. As seen in Fig. 2(b), Δn_D^{25} does not change below 4.00 wt%; however, above 5.00 wt%, Δn_D^{25} increases linearly, indicating that DNA forms a stable liquid crystal phase.

3.3. IR Spectra

The results obtained by microscopy and refractometry indicate that, in the concentration range above 5.00 wt%, an anisotropic phase appears that corresponds to the liquid crystal phase.

However, Fig. 1(d) shows a polarizing microphotograph of the phases state for solutions with 10.0 wt% DNA containing Mg^{2+} ion: the liquid crystal phase is not observed, demonstrating that its formation [15,22] may be prevented by an electrostatic interaction between the negative PO_4^- group of the main chain of DNA and the Mg^{2+} ion.

In other words, it is demonstrated that DNA molecule in concentrations above 5.00 wt% forms liquid crystals with a stable rod-like arrangement as a result of the repulsive force between the negative PO_4^- groups of the main chain of DNA.

In order to obtain further information about the effect of Mg^{2+} ion on the formation of the liquid crystal phase, IR spectra of DNA solutions with and without Mg^{2+} ion were measured at room temperature. The results obtained are shown in Fig. 3. As seen in Fig. 3, IR spectra (solid line) of DNA solutions without Mg^{2+} ion show the two bands of the symmetric stretching vibration at 1089 cm^{-1} and the anti-symmetric stretching vibration at 1226 cm^{-1} corresponding to the stretching region of phosphate groups [22,23]. However, IR spectral bands (dotted line) for DNA solution with Mg^{2+} ion shift to 1085 cm^{-1} from 1089 cm^{-1} for the symmetric stretching vibration, and to 1220 cm^{-1} from 1226 cm^{-1} for the anti-symmetric stretching vibration, respectively, demonstrating that the decrease in the stretching vibrations for the phosphate groups of the main chain of DNA in solutions containing Mg^{2+} ion may include a contribution from an electrostatic interaction between the phosphate group and Mg^{2+} ion [22]. The liquid crystal formation of DNA is inhibited by Mg^{2+} ion, and this result is compatible with that found with the polarizing microphotograph as shown in Fig. 1(d).

From these results, we suggest that the repulsive force between the negative PO_4^- groups of the main chain of DNA plays an important role in forming the liquid crystal.

3.4. Conformation of liquid crystal from CD spectra

In order to obtain information about the conformation of the liquid crystal, the circular dichroism (CD) of DNA solutions in the concentration range 1.00–10.0 wt% was also measured at room temperature. The results obtained are shown in Fig. 4. The ellipticity for DNA solutions at concentrations below 2.00 wt%, showing an isotropic phase, does not change in the wavelength region 700–400 nm. DNA solutions with a concentration of 3.00 wt%, showing a slight anisotropic phase, show a negative CD spectrum with the wavelength of the maximum reflection at 675 nm and, with further increasing DNA concentration, the wavelength of a maximum reflection shifts to lower wavelengths, demonstrating that CD spectra reflect the liquid crystal formation of DNA appearing from concentrations above 3.00 wt%. The wavelength of the

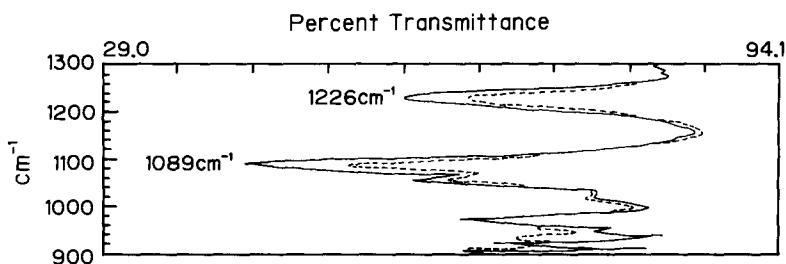


Fig. 3. IR spectra of DNA solutions of 10 wt% concentration with (---) and without Mg^{2+} ion (—).

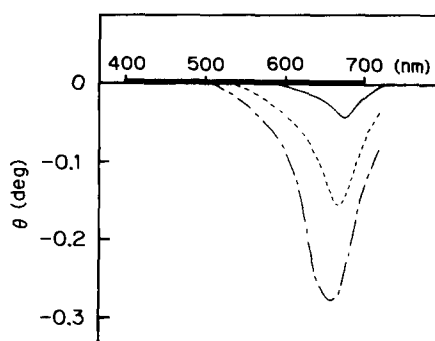


Fig. 4. CD spectra for DNA solutions of various concentrations: (—), 3.00 wt%; (.....), 5.00 wt%; (---), 10.0 wt%.

maximum reflection may be explained using the well-known equation

$$\Delta\varepsilon = \varepsilon_L - \varepsilon_R \quad (1)$$

where ε_L and ε_R are the absorption coefficients of the left and right circular polarized lights, and $\Delta\varepsilon$ is the difference between these absorption coefficients, respectively. Because the results obtained in the present work correspond to $\varepsilon_L - \varepsilon_R < 0$, DNA solutions with concentrations above 3.00 wt% correspond to a cholesteric liquid crystal with a right-handed helical sense.

However, the structural parameter characterizing the cholesteric phase is the pitch of the helical molecular arrangement. The relationship between the cholesteric pitch P and the wavelength of maximum reflection λ_{\max} can be represented as

$$\lambda_{\max} = np \quad (2)$$

where n is the average value of the refractive indices for parallel and perpendicular directions of liquid crystals of DNA. Eq. (2) is usually used for the estimation of cholesteric pitch for polypeptide and/or polyribonucleotide liquid crystalline phases [24].

Assuming that Eq. (2) can be applied in the present work, the cholesteric pitch P of cholesteric liquid crystals of DNA can be calculated in the concentration range 3.00–10.0 wt% of DNA. The results obtained are shown in Fig. 5, where P is plotted against the DNA concentration. As seen in Fig. 5, P decreases with increasing DNA concentration, demonstrating that a decrease in P forms a more stable cholesteric liquid crystal with a right-handed helical sense.

3.5. DTA equipped with laser

It is suggested that DNA in concentrated solutions forms a stable cholesteric liquid crystal with a right-handed helical sense as a result of the repulsive force between the negative PO_4^- groups of the main chain of DNA.

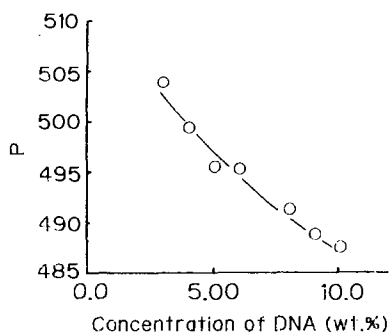


Fig. 5. Plots of the cholesteric pitch P of the cholesteric liquid crystal against various concentrations.

Furthermore, to obtain information about the change in enthalpy based on formation of the cholesteric liquid crystal, the change in enthalpy based on the order–disorder transition of the liquid crystal was estimated over the concentration range 0.05–10.0 wt% DNA from the point of view of the dissociation process from the helix–coil transition of DNA, using a differential scanning calorimeter (DSC) and a differential thermal analysis (DTA) apparatus equipped with laser which was constructed as reported previously [16,21].

Typical DSC, DTA and laser transmittance curves are shown in Fig. 6 (a)– (d). The DTA curves obtained over the concentration range 1.00–10.0 wt% exhibit two endothermic peaks around 333 and 350 K, except for the DSC curve for the 0.05 wt% DNA solution (Fig. 6 (a)). The endothermic DTA peak at 333 K has a constant value which is nearly independent of the DNA concentration. However, the peak at around 350 K shifts to higher temperatures with increasing DNA concentration. In order to confirm the endothermic DTA peak, DSC measurement for 0.05 wt% DNA was carried out, see Fig. 6(a), in which the DSC curve shows a characteristic endothermic peak corresponding to the usual helix–coil transition of DNA in dilute solution.

In addition, it is interesting that the complicated shoulder peaks seen in Fig. 6(a) show the characteristic base sequences of calf thymus DNA [25].

From DSC measurements in dilute solution, it can be concluded that the endothermic peaks of the DTA curves at 353–366 K correspond to the phase transitions taking place at the same time, e.g. the helix–coil transition and the order–disorder transition of the cholesteric liquid crystal. Because an endothermic peak on the DSC curve corresponding to the lower temperature of the DTA curve does not appear in dilute solution (Fig. 6(a)), a broad endothermic DTA peak at lower temperatures in the vicinity of 333–343 K observed with increasing DNA concentration may correspond to the change in enthalpy, based on a spread of the cholesteric pitch P with increasing temperature, because P increases with an increase in temperature, as seen from the temperature dependence of CD spectra as shown in Fig. 7. Thus, the molecular orientation of the cholesteric liquid crystal transforms gradually into the disorder structure. However, the change in intensity of transmitted laser light increases slightly with increasing temperature. In the concentration range 1.00–10.0 wt%, the intensity of the laser transmittance increases considerably corresponding to the beginning of the

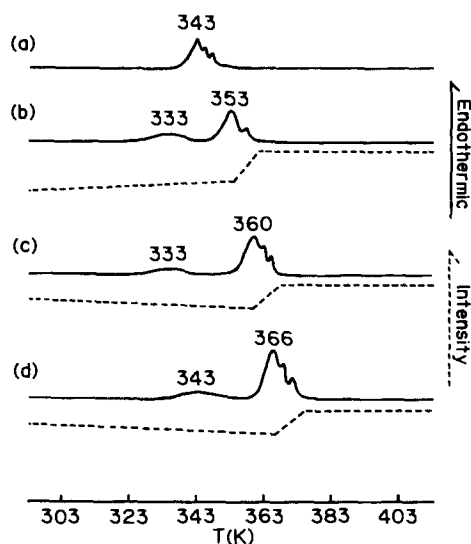


Fig. 6. (a) Typical DSC and (b), (c) DTA–laser transmittance curves for DNA solutions of various concentrations. DTA and DSC curves are presented as solid lines and the laser transmittance curve is presented as a dotted line, respectively. DNA concentrations: (a) 0.05 wt%; (b) 1.00–2.00 wt%; (c) 3.00–5.00 wt%; (d) 6.00–10.0 wt%.

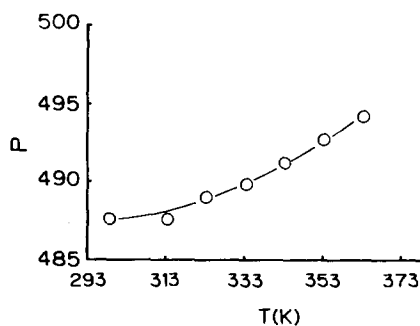


Fig. 7. Temperature dependence of the cholesteric pitch P of the cholesteric liquid crystal for 10.0 wt% DNA solution.

endothermic peak representing the helix–coil transition of DNA at higher temperatures, with increasing temperature.

To confirm the change in the intensity of transmitted laser light corresponding to the beginning of thermal change around 353–366 K, the phase state for the 10.0 wt% DNA solution was observed using a polarization microscope equipped with a hot stage. The polarizing micro-photographs for the change in phase states corresponding to the changes in the DTA and laser transmittance curves are shown in Fig. 8. The disappearance of the cholesteric liquid crystal can be observed in the polarizing microphoto-

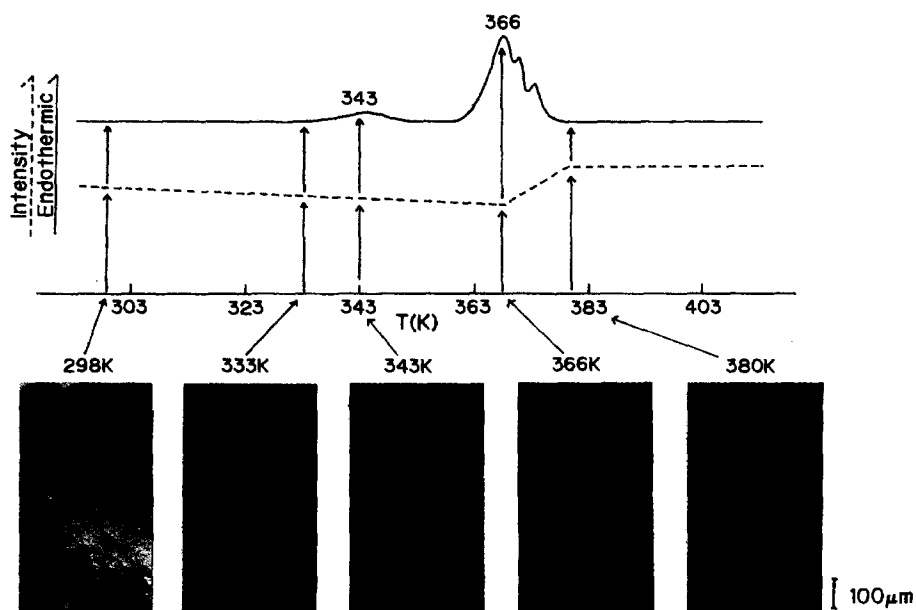


Fig. 8. Thermograms of the DTA-laser transmittance curves corresponding to phase state observed from the polarizing microphotographs with increasing temperature.

graphs corresponding to a broad endothermic peak in the neighborhood of 343 K, which corresponds to the change in enthalpy based on a spread of the cholesteric pitch, as pointed out in Fig. 7. This tendency is similar to that of the temperature dependence of the UV spectra of T7 phage reported by Ronto [26] and the small-angle X-ray scattering experiment of T7 phage reported by Dembo et al. [27] and Fekete et al. [28].

From the polarizing microphotograph for the phase state corresponding to the beginning of the endothermic DTA peak at 366 K, this endothermic peak corresponds to the change in enthalpy based on the order–disorder transitions of the cholesteric liquid crystal and the simultaneous helix–coil transition of DNA, and transforms into an isotropic phase (coiled phase) with an increase in temperature. However, the intensity of the transmitted laser light corresponding to the start of the thermal change of the cholesteric liquid crystal phase at higher temperatures increases with increasing temperature. A possible explanation for this behavior is as follows. The behavior seems to be a result of the cooperative action between the increase in the intensity of transmitted light accompanying the disorder of the cholesteric liquid crystal and the decrease in the intensity of transmitted laser light by an increase in the scattered light accompanying the change in DNA from a helical conformation to a coiled one [14] with increasing temperature. It is suggested that the change in intensity of the transmitted light accompanying the change in phase state reflects the molecular conformation in the phase state of the cholesteric liquid crystal with increasing temperature.

3.6. Change in enthalpy of cholesteric liquid crystal

Assuming that the endothermic peak of the DTA curve at higher temperatures corresponds to the phase transition of the cholesteric liquid crystal, the transition temperature T , from the endothermic peak, and the change in enthalpy ΔH , from the area of the DTA curve using the change in enthalpy of the standard samples as described in the experimental section, can be determined.

The results obtained are shown in Fig. 9(a) and (b), where T_1 is the transition temperature at lower temperatures, T_2 is the transition temperature based on the helix–coil transition and the order–disorder transition of the cholesteric liquid crystal at higher temperatures, and ΔH_1 and/or ΔH_2 are the changes in enthalpy corresponding to T_1 and T_2 , respectively.

As seen in Fig. 9(a), T_1 at DNA concentrations below 5.00 wt% is constant and virtually independent of DNA concentration. However, at concentrations above 6.00 wt%, T_1 increases, reflecting the more stable liquid crystal phase in comparison with T_1 for concentrations below 5.00 wt% from the polarization microscopic results. T_2 at concentrations above 6.00 wt% reflects a more stable liquid crystal formation similar to that of T_1 in this concentration range. It is suggested that the concentration of 6.00 wt% corresponds to the critical concentration for forming the stable cholesteric liquid crystal, from the results of T_1 , T_2 and the birefringence.

However, as seen in Fig. 9(b), ΔH_1 shows a definite value which is nearly independent of the DNA concentration and can be estimated graphically as about 1.0 kJ per mole of base pair of DNA. However, ΔH_2 at higher temperatures shows a definite value by 5.00

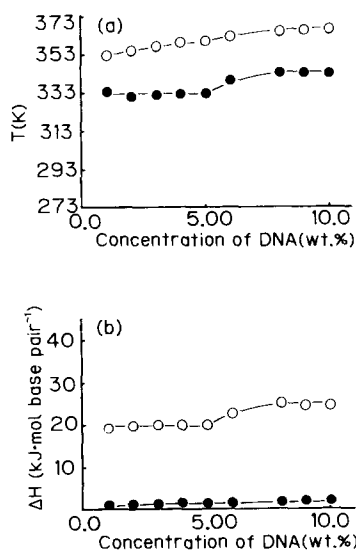


Fig. 9. Plots of (a) transition temperatures T_1 (●) at lower temperatures and T_2 (○) at higher temperatures, and (b) the transition enthalpy ΔH_1 (●) and ΔH_2 (○) corresponding to T_1 and T_2 against DNA concentration.

wt%, and is then asymptotic to $\Delta H_2 = 25$ kJ per mole of base pair from concentrations above 6.00 wt%, suggesting that this ΔH_2 value corresponds to the change in enthalpy based on the order–disorder phase transition of the cholesteric liquid crystal and the helix–coil transition of DNA taking place at the same time.

3.7. Degree of order α of liquid crystal

Assuming that the change in intensity of transmitted laser light over the concentration range 1.00–10.0 wt% corresponding to the start of thermal change in the DTA curve at higher temperatures is related to the degree of order–disorder α of the cholesteric liquid crystal, α can be estimated from the change in intensity of the transmitted laser light. The difference ΔI between before and after the changes from the base line of the laser transmittance curve for the intensity of the transmitted laser light with increasing temperature is related to the α value of the cholesteric liquid crystal for each DNA concentration.

The results obtained are shown in Fig. 10, where ΔI is plotted against the DNA concentration. As seen in Fig. 10, ΔI decreases at first and reaches a constant value with increasing DNA concentration, demonstrating that the decrease in ΔI corresponds to the increase in α of the cholesteric liquid crystal phase. The behavior of ΔI is comparable with that of DNA observed from the DTA curve, polarization microscope and birefringence. The value of α can be estimated from the behavior of ΔI as follows. The conformation of DNA over the concentration range 1.00–10.0 wt% is assumed to lead to the coiled conformation from the helical one with increasing temperature. On the basis of this coiled conformation, the intensity I_c for the coiled conformation and I_h for the helical one are related as

$$I_c = I_o \exp(-\varepsilon^c cd) \quad (3)$$

and

$$I_h = I_o \exp(-\varepsilon^h cd) \quad (4)$$

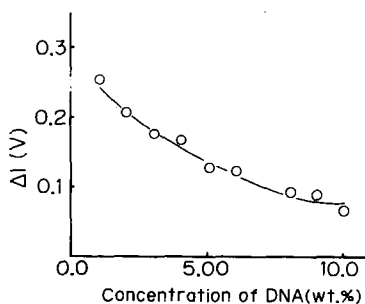


Fig. 10. Plots of the difference ΔI (V) before and after changes from the base line of the laser transmittance curve against DNA concentration (wt%).

where ε^c and ε^h are the scattered coefficients per weight for the coiled and helical conformations, respectively, c is the DNA concentration (wt%), and the light-path length d has a fixed value under the present experimental conditions.

The difference between Eqs. (3) and (4) gives the change in molecular conformation of DNA with increasing concentration.

Taking the logarithm of both sides of Eqs. (3) and (4), and subtracting Eq. (4) from Eq. (3)

$$(\ln I_c - \ln I_h) = -\Delta\varepsilon cd \quad (5)$$

where $\Delta\varepsilon = \varepsilon^c - \varepsilon^h$.

According to Eq. (5), a plot of $(\ln I_c - \ln I_h)$ against c is shown in Fig. 11(a). If all phase states exist as isotropic phases, this plot would give a straight line, as shown in the dotted line of Fig. 11(a). However, as seen in Fig. 11(a), the experimental points at $c > 3.00$ wt% show deviation from the calculated value (dotted line), which corresponds to the conformational change based on the order–disorder transition of the cholesteric liquid crystal. And then, it must be corrected for the deviation which contributes to the formation of the cholesteric liquid crystal. The corrected term $\varepsilon^{\text{Form}}$, for the scattered light based on formation of the cholesteric liquid crystal, must be added to ε^h in Eq. (4), and then Eq. (5) is modified to

$$(\ln I_c - \ln I'_h) = -\Delta\varepsilon' cd \quad (6)$$

where $I'_h = I_o \exp[-(\varepsilon^h + \varepsilon^{\text{Form}}) cd]$ and $\Delta\varepsilon' = \varepsilon^c - (\varepsilon^h + \varepsilon^{\text{Form}})$, respectively.

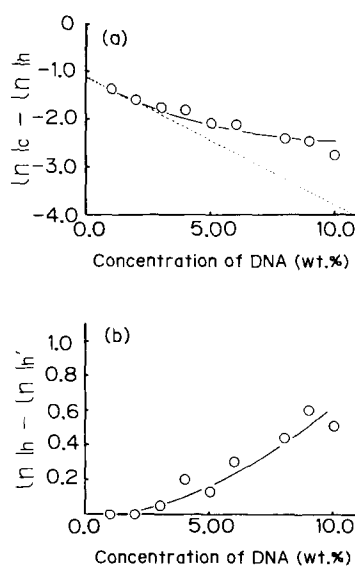


Fig. 11. Plots of (a) $\ln I_c - \ln I_h$, and (b) $\ln I_c - \ln I'_h$ against DNA concentration (wt%) according to Eqs. (5) and (7), respectively.

Accordingly, the effect of the cholesteric liquid crystal formation can be estimated by subtracting Eq. (5) from Eq. (6)

$$(\ln I_h - \ln I'_h) = \varepsilon^{\text{Form}}cd \quad (7)$$

According to Eq. (6), a plot of $(\ln I_h - \ln I'_h)$ against c is shown in Fig. 11(b): $(\ln I_h - \ln I'_h)$ increases considerably with an increasing c although the values are somewhat scattered, suggesting that an increase in $(\ln I_h - \ln I'_h)$ corresponds to an increase in the formation of the cholesteric liquid crystal with increasing c .

In Fig. 11(b), assuming that the $(\ln I_h - \ln I'_h)$ value at 10.0 wt% DNA concentration forms the cholesteric liquid crystal perfectly, the α value for each DNA concentration can be presented as the ratio of $(\ln I_h - \ln I'_h)$ to $\lim_{c \rightarrow 10.0 \text{ wt}\%} (\ln I_h - \ln I'_h)$ as

$$\alpha = \frac{(\ln I_h - \ln I'_h)}{\lim_{c \rightarrow 10.0 \text{ wt}\%} (\ln I_h - \ln I'_h)} \quad (8)$$

According to Eq. (8), α can be determined and the results obtained are listed in the second column of Table 1.

The change in enthalpy ΔH_d , based on the order–disorder transition of the cholesteric liquid crystal for each DNA concentration, can be determined using α values listed in Table 1.

3.8. Change in net enthalpy of formation of cholesteric liquid crystal

Again as shown in Fig. 9(b), the observed heat ΔH_2 at higher temperatures can be assumed to be the sum of the change in enthalpy based on the helix–coil transition ΔH_t and $\alpha \Delta H_d$, based on the order–disorder of the cholesteric liquid crystal, by taking into

Table 1

The change in enthalpy ΔH_d based on the order–disorder transition of the cholesteric liquid crystal by considering the degree of disorder α of the cholesteric liquid crystal of DNA

| Conc. of DNA/wt% | α | $\Delta H_d/(\text{kJ mol}^{-1})^a$ |
|------------------|----------|-------------------------------------|
| 1.00 | 0.0 | 0.0 |
| 2.00 | 0.0 | 0.0 |
| 3.00 | 0.10 | – |
| 4.00 | 0.39 | 1.1 |
| 5.00 | 0.26 | 1.6 |
| 6.00 | 0.59 | 2.9 |
| 8.00 | 0.96 | 3.5 Ave. ^b |
| 9.00 | 1.00 | 2.2 2.8 |
| 10.0 | 1.00 | 2.7 |

^a Mol is mole of nucleotide of DNA.

^b The net ΔH_D value estimated as the average value at concentrations above 6.00 wt% of DNA.

consideration the value of α

$$\Delta H_2 = \Delta H_t + \alpha \Delta H_d \quad (9)$$

Therefore, ΔH_d can be estimated from $(\Delta H_2 - \Delta H_t)/\alpha$. The results obtained in such a way are summarized in the last column of Table 1 and are also shown in Fig. 12, where ΔH_d is plotted against $c(\text{wt}\%)$.

As seen in Fig. 12, ΔH_d increases at first and then is asymptotic to $\Delta H_d = 2.8 \text{ kJ}$ with an increase of $c(\text{wt}\%)$, demonstrating that this value gives the change in net enthalpy ΔH_D , based on the order–disorder transition of the cholesteric liquid crystal of DNA.

However, because the ΔH_D value cannot be exactly determined graphically due to scatter, ΔH_D is estimated to be about 2.8 kJ per mole of nucleotide as an average value of ΔH_d at concentrations above 6.00 wt% listed in the last column of Table 1.

It is suggested that the reverse sign of ΔH_D estimated above corresponds to the change in net enthalpy, ΔH_F ($= -2.8 \text{ kJ}$), based on the cholesteric liquid crystal formation of DNA.

4. Conclusion

In order to obtain information about the mechanism of the liquid crystal formation and the change in enthalpy, DNA was studied in concentrated solutions by means of DTA equipped with a laser, spectrophotometry, a polarization microscope, and the refractive index.

From these results, it has been concluded that DNA in concentrated solutions forms a cholesteric liquid crystal with a right-handed-helical sense as a result of the repulsive force between the negative PO_4^- groups of the main chain of DNA as evidenced from CD measurement and from the fact that the liquid crystal formation of DNA is inhibited by an electrostatic interaction between the PO_4^- group and Mg^{2+} ion, as demonstrated in the experimental IR spectra. Furthermore, the change in net enthalpy based on formation of the cholesteric liquid crystal has been estimated to be about -2.8 kJ per mole of nucleotide by taking into consideration the value of α estimated from the change in intensity of transmitted laser light with increasing DNA concentration.

References

- [1] K. Fujioka, Y. Baba and A. Kagemoto, *Polym. J.*, 11 (1979) 509.
- [2] A. Kagemoto, H. Irie, M. Aramata and Y. Baba, *Thermochim. Acta*, 181 (1991) 155.
- [3] Y. Matsuoka, A. Nomura, S. Tanaka, Y. Baba and A. Kagemoto, *Thermochim. Acta*, 163 (1990) 147.
- [4] Y. Baba and A. Kagemoto, *Biopolymers*, 13 (1974) 339.
- [5] K. Kano, Y. Baba and A. Kagemoto, *Thermochim. Acta*, 88 (1985) 323.
- [6] K. Kanoh, Y. Baba and A. Kagemoto, *Polym. J.*, 20 (1988) 1135.
- [7] S. Tanaka, Y. Baba, A. Kagemoto and R. Fujishiro, *Makromol. Chem.*, 181 (1980) 2175.
- [8] Y. Baba, C.L. Beatty and A. Kagemoto, *Biological Activities of Polymers*, ACS Symposium Series, 186 (1982) 177.

- [9] W. C. Earnshaw and S.R. Casjens, *Cell*, 21 (1980) 319.
- [10] T. E. Strzelecka and R.L. Rill, *Biopolymers*, 30 (1990) 57.
- [11] T. E. Strzelecka, M.W. Davidson and R.L. Rill, *Nature*, 331 (1988) 457.
- [12] C. Robinson, *Tetrahedron*, 13 (1961) 219.
- [13] E. Iizuka, *Polym. J.*, 9 (1977) 173.
- [14] D.H. Van Winkle, M.W. Davidson, W.X. Chen and R.L. Rill, *Macromolecules*, 23 (1990) 4140.
- [15] T.E. Strzelecka and R.L. Rill, *Macromolecules*, 24 (1991) 5124.
- [16] A. Kagemoto, Y. Okada, H. Irie, M. Oka and Y. Baba, *Thermochim. Acta*, 176 (1991) 1.
- [17] E. Iizuka and J.T. Yang, *Liquid Crystals and Ordered Fluids*, Plenum press, New York, 3 (1978) 197.
- [18] E. Senechal, G. Maret and K. Dransfeld, *Int. J. Biol. Macromol.*, 2 (1980) 256.
- [19] J. Sambrook, E.F. Fritsch and T. Maniatis, *Molecular Cloning — A Laboratory Manual*, 2nd edn., Cold Spring Harbor Laboratory Press, New York, 1989.
- [20] P. S. Chen, T.Y. Toribara and H. Warner, *Anal. Chem.*, 28 (1956) 1756.
- [21] M. Kyoumen, Y. Baba, A. Kagemoto and C.L. Beatty, *Macromolecules*, 23 (1990) 1085.
- [22] M. Langlais, A. Tajmir-Riahi, R. Savoie, *Biopolymers*, 30 (1990) 743.
- [23] G.B.B.M. Sutherland and M. Tsuboi, *Proc. R. Soc. London Ser. A*, 239 (1957) 446.
- [24] E. Iizuka, *Polym. J.*, 10 (1978) 293.
- [25] N. Fujita, K. Ueno, M. Satoh, S. Kimura, Y. Baba and A. Kagemoto, *Rep. Prog. Polym. Phys. Jpn.*, 36 (1993) 689.
- [26] G. Ronto, *Acta Biochim. Biophys. Acad. Sci. Hung.*, 19 (1984) 221.
- [27] A.T. Dembo, A. Fekete Gy. Ronto and V.V. Tikhonchev, *Stud. Biophys.*, 87 (1982) 279.
- [28] A. Fekete, Gy. Ronto, L.A. Feigin, V.V. Tikhonchev and K. Modos, *Biophys. Struct. Mech.*, 9 (1982) 1.